ACS APPLIED MATERIALS & INTERFACES

Research Article

www.acsami.org

Improving Polymer/Nanocrystal Hybrid Solar Cell Performance via Tuning Ligand Orientation at CdSe Quantum Dot Surface

Weifei Fu,[†,⊥] Ling Wang,[†,⊥] Yanfang Zhang,[‡] Ruisong Ma,[‡] Lijian Zuo,[†] Jiangquan Mai,[§] Tsz-Ki Lau,[§] Shixuan Du,[‡] Xinhui Lu,[§] Minmin Shi,[†] Hanying Li,*[,†] and Hongzheng Chen*[,†]

[†]State Key Laboratory of Silicon Materials, MOE Key Laboratory of Macromolecular Synthesis and Functionalization, Department of Polymer Science and Engineering, Zhejiang University, Hangzhou 310027, People's Republic of China

[‡]Institute of Physics, Chinese Academy of Sciences, Beijing 100190, People's Republic of China

[§]Department of Physics, Chinese University of Hong Kong, New Territories, Hong Kong, People's Republic of China

Supporting Information

ABSTRACT: Achieving superior solar cell performance based on the colloidal nanocrystals remains challenging due to their complex surface composition. Much attention has been devoted to the development of effective surface modification strategies to enhance electronic coupling between the nanocrystals to promote charge carrier transport. Herein, we aim to attach benzenedithiol ligands onto the surface of CdSe nanocrystals in the "face-on" geometry to minimize the nanocrystal−nanocrystal or polymer−nanocrystal distance. Furthermore, the "electroactive" π-orbitals of the benzenedithiol are expected to further enhance the electronic coupling, which facilitates charge carrier dissociation and transport. The electron mobility of CdSe QD films was improved 20 times by tuning the ligand orientation, and high performance poly[2,6-(4,4-bis(2-ethylhexyl)-4H-cyclopenta[2,1-b;3,4-b′]-dithiophene)-*alt*-4,7-(2,1,3-benzothiadiazole)] (PCPDTBT):CdSe nanocrystal hybrid solar cells were also achieved, showing a highest power conversion efficiency of 4.18%. This research could open up a new pathway to improve further the performance of colloidal nanocrystal based solar cells.

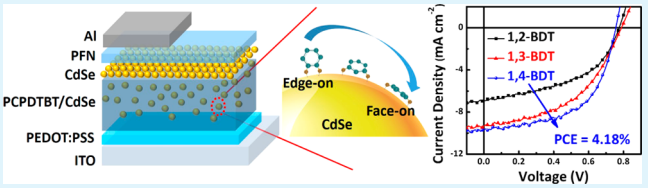

KEYWORDS: *hybrid solar cell, ligand orientation, electronic coupling, exciton dissociation, charge transport*

1. INTRODUCTION

Colloidal nanocrystals offer the potentialities and have been demonstrated for low-cost and solution-processed electronic device applications such as field-effect transistors,[1,2] light-emitting diodes[3,4] and photovoltaics,[5−13] due to their spectral tunability via quantum confinement effect and potentially high charge carrier mobilities. However, achieving superior device performance remains challenging due to the complex surface composition and (opto) electronic behavior of the nanocrystals. Nanocrystals are generally capped with long chain organic ligands to ensure their solution process ability, following their synthesis in solution.[14−21] When the nanocrystals are processed into films, these insulating ligands militate against efficient exciton dissociation and carrier transport, which is detrimental to the device performance. Therefore, much attention has been devoted to the development of effective surface modification strategies to enhance the electronic coupling between the nanocrystals by replacing the pristine ligands with shorter ligands to promote carrier transport while passivating the nanocrystal surface to limit recombination loss.[5,6,22−32]

Thiols are the widely used, as postdeposition surface modification ligands, for polymer/nanocrystals hybrid solar cells (HSCs) due to their strong affinity to the nanocrystals, which can replace the X-type ligands nearly completely.[22,33−35] A power conversion efficiency (PCE) of 3.09% was obtained in our lab after surface modification by *n*-butanethiol for poly(3-hexylthiophene) (P3HT):CdSe quantum dots (QDs) HSCs.[33] Metal chalcogenide complexes have emerged as promising materials to effectively remove the pristine ligands, enhancing strong electronic coupling between nanocrystals in films,[2,36] and impressive field-effect transistor (FET) electron mobilities up to 16 $cm^2\ V^{-1}\ s^{-1}$ were obtained in $In_2Se_2^{4-}$ capped CdSe QDs.[1] Atomic ligands such as halide, chalcogenides and hydrochalcogenides are also used to passivate the nanocrystal surface with the goal of using the shortest imaginable ligands.[2,6,23,37] All these works indicate that minimizing the distance between the chalcogenide nanoparticles and/or the polymer−nanocrystal is crucial for device performance and the nonelectroactive insulating ligands should be removed as much as possible. The atomic ligand passivation strategy was widely used in quantum dot solar cells.[5,6] However, seldom successful work was reported for polymer/nanocrystal hybrid solar cells involving atomic ligand. When trying to introduce the atomic ligands for post deposition ligand exchange, we found that the blend films will be destroyed by the atomic ligand/acetonitrile solution. Considering to the different solubilities of the atomic

Received: August 1, 2014
Accepted: October 22, 2014
Published: October 22, 2014

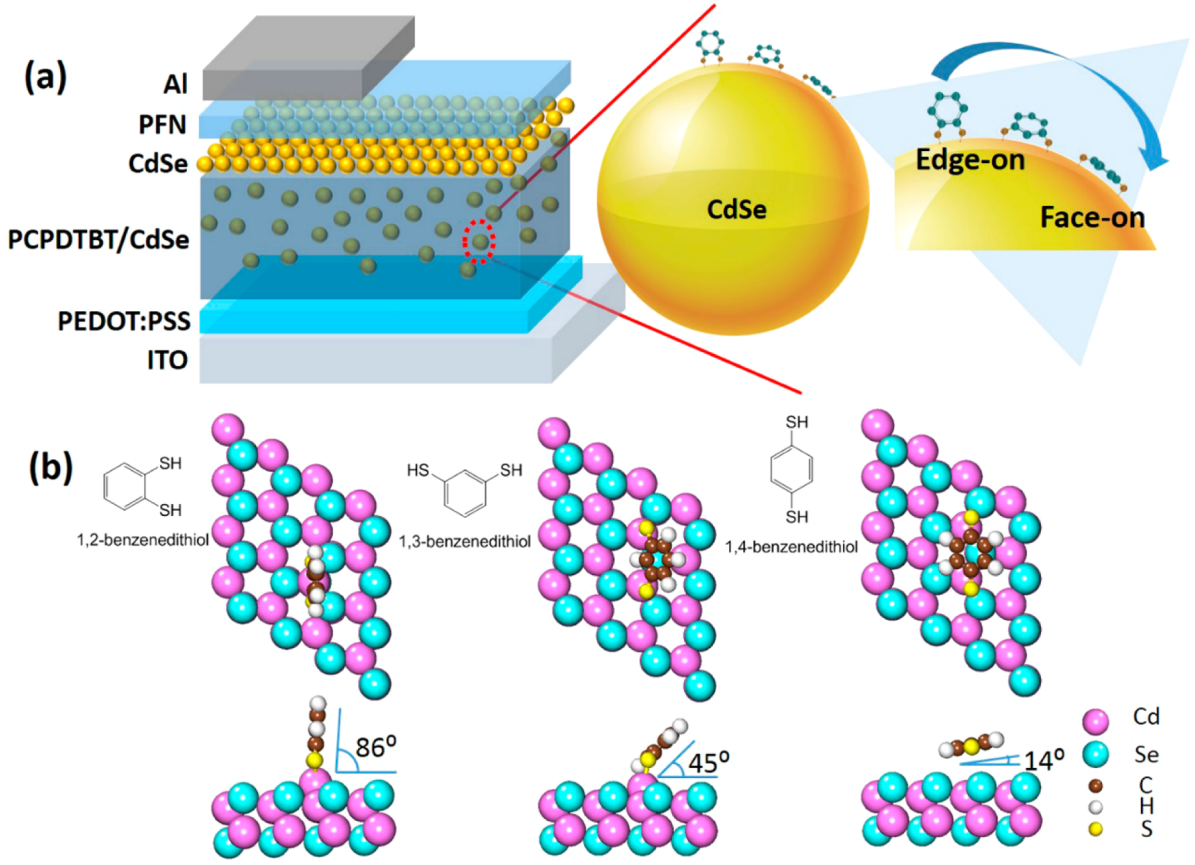

Figure 1. (a) Schematic device structure used in this study and the schematic illustration of orientation of various benzenedithiols on the surface of CdSe QDs. (b) Density functional theory (DFT) calculation results showing the orientation of the various benzenedithiols on the CdSe (0001) surface. 1,4-Benzenrdithiol lays its electrostatically "reactive" π-orbitals on the surface of the CdSe QDs, while the 1,2-benzenedithiol shields its π-orbitals from the surface.

ligand treated nanocrystal and polymer, the idea about blending atomic ligand treated nanocrystal and polymer was also failed. So some new and different ligand exchange strategies should be developed with the idea of enhancing the electronic coupling between polymer and nanocrystal in mind.

Following this strategy, we aim to further increase the performance of the polymer/CdSe QDs hybrid solar cells by attaching benzenedithiol (BDT) ligands on the surface of CdSe nanocrystals in the "face-on" geometry to minimize the nanocrystal−nanocrystal or polymer−nanocrystal distance. Furthermore, the "electroactive" π-orbitals of the benzenedithiol ligands are expected to further enhance the electronic coupling between nanocrystals or between polymer and nanocrystals, facilitating charge carrier dissociation and transport. This was successfully done by simply selecting benzenedithiols with −SH groups that are substituted in different positions. By tuning the ligand orientation, the electron mobility of CdSe QD film was improved 20 times, and high performance poly[2,6-(4,4-bis(2-ethylhexyl)-4H-cyclopenta[2,1-b;3,4-b′]-dithiophene)-*alt*-4,7-(2,1,3-benzothiadiazole)] (PCPDTBT):CdSe QDs HSCs were also achieved, showing a highest PCE of 4.18%, with short-circuit current density (J_{sc}) of 9.69 mA cm^{-2}, open-circuit voltage (V_{oc}) of 0.76 V and fill factor (FF) of 0.568. To our knowledge, this PCE value is among the highest ever reported for CdSe QDs based HSCs.

2. EXPERIMENTAL SECTION

CdSe QDs Synthesis. CdSe QDs were synthesized according to the reported procedure.[38] In a typical synthetic process, CdO (76 mg), trioctylphosphine oxide (TOPO, 3.0 g) and oleic acid (OA, 3.0 mL) were added into the reactor and the mixture was heated to 285 °C under vigorous stirring in nitrogen atmosphere. Se (80 mg) was added into trioctylphosphine (TOP, 1.0 mL), and the mixture was sonicated until the solution became clear. Then the Se-TOP solution was quickly injected into the reactor. 5 min later, the hot solution was quickly transferred into toluene (5 mL). The as-prepared CdSe QDs were washed in methanol and centrifuged for two times and then dispersed in pyridine (15 mL), and the mixture was stirred for 24 h. The resulting nanocrystals were flocculated by hexane and centrifuged.

Device Fabrication and Testing. Prior to fabrication, the substrates were cleaned by sonication using detergent, deionized water, acetone and isopropyl alcohol sequentially for every 15 min followed by 15 min of ultraviolet ozone (UV-ozone) treatment. Then a layer of poly(3,4-ethylenedioxythiophene):poly(styrenesulfonate) (PEDOT:PSS) (Baytron P AI4083) was spin-coated onto the cleaned ITO and baked in air at 140 °C for 15 min. Then the substrates were transferred to a glovebox for spin coating of a PCPDTBT:CdSe QDs (1:9, w/w) active layer with a thickness of about 90 nm. The postdeposition ligand-exchange process was carried out by soaking the as-prepared films in a solution of 10 mM benzenedithiol or toluenethiol in acetonitrile for 30 s, then rinsed with pure acetonitrile twice to remove the excess benzenethiol or toluenethiol and OA. Subsequently, a thin pure nanocrystal layer was deposited onto the blend film from a 5 mg mL^{-1} CdSe QDs solution in hexane, then ligand exchanged and cleaned as described above. Subsequently, 5 nm PFN film was deposited on the active layer as a cathode buffer layer. Then the samples were loaded into a vacuum deposition chamber

(background pressure ≈ 5×10^{-4} Pa) to deposit 100 nm thick Al as cathode with a shadow mask (device area of 5.2 mm^2). The $J-V$ curves were measured with Keithley 2400 measurement source units at room temperature in air. The photocurrent was measured under a calibrated solar simulator (Abet 300 W) at 100 mW cm^{-2} under standard AM 1.5G conditions in air, and the light intensity was calibrated with a standard photovoltaic reference cell. The EQE spectrum was measured with Stanford lock-in amplifier 8300 unit.

Characterization. The XPS was measured in an integrated ultrahigh vacuum system equipped with multitechnique surface analysis system (Thermo ESCALAB 250Xi). The steady-state PL spectra were taken on a FluoroMax-4 HORIBA Jobin Yvon spectrofluorometer.

3. RESULTS AND DISCUSSION

HSCs based on PCPDTBT:CdSe QDs with various benzenedithiols at the polymer/nanocrystal interface were fabricated with device structure of ITO/poly(3,4-ethylenedioxythiophene):polystyrenesulfonic acid (PEDOT:PSS)/PCPDTBT:CdSe QDs/poly[(9,9-bis(3′-(*N*,*N*-dimethylamino)propyl)-2,7-fluorene)-*alt*-2,7-(9,9-dioctylfluorene)] (PFN)/Al, as shown in Figure 1a. A postdeposition ligand exchange treatment was applied, using 1,2-benzenedithiol (1,2-BDT), 1,3-benzenedithiol (1,3-BDT) or 1,4-benzenedithiol (1,4-BDT) dissolved in anhydrous acetonitrile, to treat the hybrid PCPDTBT/CdSe QD films in which the QDs were capped with oleic acid and pyridine with the size of ~6 nm (Figure S1, Supporting Information). This method helps us to graft the benzenedithiols on the nanocrystal surface with different configurations. Schematic illustration of the surface chemistry of CdSe QDs is shown in Figure 1a. Due to the strong affinity of thiols with Cd^{2+} on the surface of CdSe QDs, which are postulated to replace the X-type ligands by forming Cd-thiolate,[22] both −SH groups of the same BDT molecule anchor on the surface of the nanocrystals, which is demonstrated by Fourier transform infrared spectroscopy (FTIR) and X-ray photoelectron spectroscopy (XPS) (Figures S2 and S3, Supporting Information, respectively). Thus, the orientations of the three benzenedithiols can be schematically illustrated in Figure 1a in a simple qualitative steric point of view. The benzene ring of 1,4-BDT will be closer to the surface of CdSe QDs in the case of face-on orientation as compared to the other two orientations with 1,2-BDT and 1,3-BDT ligands.

Density functional theory (DFT) calculations were employed to further explore the orientation of different benzenedithiols on the CdSe QD surface, using the Viena ab initio simulation package (VASP).[39,40] Because the geometric size of the CdSe QDs is drastically larger than that of the benzenedithiol molecules, for simplicity, a two-layer slab model of CdSe(0001) surface was used instead of a spherical shape. Generalized gradient approximation (GGA) in the form proposed by Perdew, Burke and Ernzerhof (PBE)[41] was used to express the exchange-correlation energy of interaction among electrons, while the frozen-core projector augmented wave method[42] was used to illustrate the interaction between ions and electrons. The plane wave kinetic energy cutoff is set to 400 eV. The convergence criterion of the total energy is 10^{-4} eV, and the maximum residual force allowed on each atom is 0.01 eV/Å. The calculation results are shown in Figure 1b. As for the 1,2-BDT molecule, the S atom forms a covalent bond with a Cd atom present on the surface of the CdSe(0001) nanoparticle, and the entire molecule is almost perpendicular to the CdSe(0001) surface and it is titled by 4° from the surface normal, i.e., an edge-on orientation, shielding its π-orbitals from the CdSe(0001) surface. On the other hand, 1,4-BDT almost lies flat on the CdSe(0001) surface with a tilting angle of 14° from the QD surface in the face-on orientation, whereas 1,3-BDT has an intermediate tilting angle of 45° from the QD surface. These results are consistent with the previous works on benzenethiols adsorption on the surface of Ag or Au.[43,44] The interaction between π-orbitals of the ligand and the surface may be significant in the 1,4-BDT case with face-on orientation.[43] Hence, a comprehensive modeling, taking into account the curvature effect, the presence of nearby particles and intercrystal binding will provide more accurate information about the BDT binding modes.[5,45] However, it is beyond the scope of this manuscript. For the effect of internanocrystals connection, Sargent et al. employed grazing-incidence small-angle X-ray scattering (GISAXS) to measure the interparticle distance of PbS nanocrystal films and found that mercaptopropionic acid, a bidentate organic cross-linker, can reduce the average center-to-center nanocrystal distance by cross-linking in the pure PbS films.[5] Here, GISAXS measurements were also carried out at beamline 16B1 in shanghai synchrotron radiation facility. No obvious change was observed in interparticle distance for blend films treated by various BDTs (Figure S4, Supporting Information). It indicated that the device performance differences induced by inter nanocrystals connection can be ignored.

Cofacial and strong π-stack interaction between the molecules results in very efficient electronic coupling, which is a promising route to increase carrier mobilities in organic semiconductors.[46,47] To make a realistic evaluation on the effect of ligand orientation on charge transport properties of CdSe QDs films, we measured the current density−voltage ($J-V$) characteristics of electron-only devices in configuration of ITO/PFN/CdSe QDs/PFN/Al and the carrier mobility was extracted by fitting the $J-V$ characteristics using the space-charge-limited current (SCLC) model (Figure 2) and the Mott−Gurney law, given by

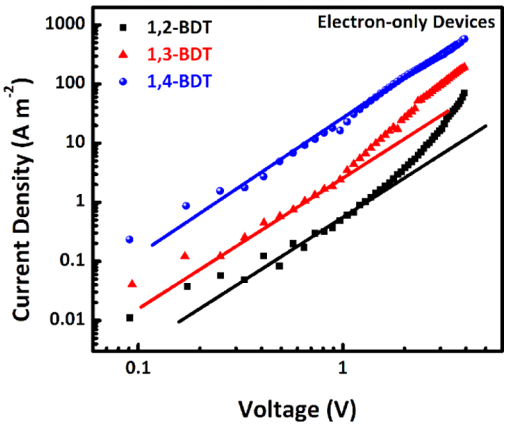

Figure 2. Effect of ligand orientation on charge transport properties of neat CdSe QDs film. $J-V$ characteristics of electron-only device in configuration of ITO/PFN/CdSe QDs/PFN/Al.

$$J = \frac{9}{8}\varepsilon_0\varepsilon_r\mu\frac{V^2}{L^3}$$

where $\varepsilon_0\varepsilon_r$ (ε_r = 6 here[48]) is the dielectric permittivity of the CdSe QDs film, L is the thickness of the film and V is the applied voltage. It clearly envisages that the electron mobility is

completely depending on the orientation of benzene ring to the CdSe QDs, i.e., increases from $(1.4 \pm 0.7) \times 10^{-7}$ to $(7.8 \pm 3.8) \times 10^{-7}$ cm^2 V^{-1} s^{-1} and further to $(3.0 \pm 1.1) \times 10^{-6}$ cm^2 V^{-1} s^{-1} for 1,2-BDT, 1,3-BDT and 1,4-BDT modified nanocrystal films, respectively. These results suggest that the face-on orientated benzene ring could greatly improve the charge transport properties, which is beneficial for achieving high performance HSCs. This improvement arises from an enhanced electronic coupling between the nanocrystals and the π-orbitals of benzene ring when it takes face-on orientation.

The absorption spectra of the neat CdSe QD films and PCPDTBT/CdSe hybrid films with various QD surface treatment/capping are shown in Figure 3a. The absorption of

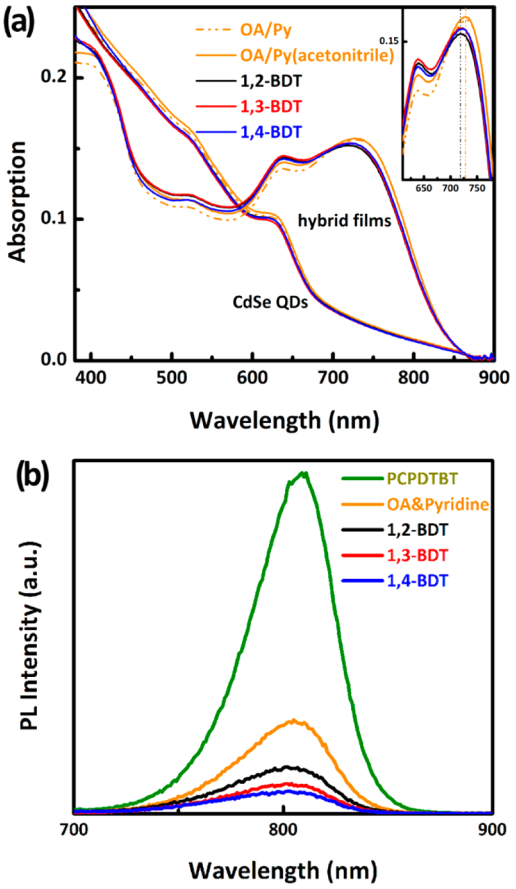

Figure 3. (a) Absorption spectra of the neat CdSe QD films and PCPDTBT/CdSe QDs blend films with different treatments. (b) PL spectra of the neat PCPDTBT film and PCPDTBT/CdSe QDs blend films with different benzenedithiols at polymer/nanocrystal interface.

CdSe QD film was nearly the same with different ligands on the QD surface, whereas the benzenedithiols slightly blue-shifted the PCPDTBT absorption spectra from 729 to 719 nm. Because acetonitrile, which is the solvent for BDT alone, cannot alter the absorption of the polymer, we infer that this may be due to the loosening of the molecular packing of the polymer chain with the increased space at the polymer/nanocrystal interface induced by the removal of bulky surfactants. Steady-state photoluminescence (PL) measurements were conducted to study the exciton dissociation process with different benzenedithiols at the donor/acceptor (D/A) interface. As shown in Figure 3b, PCPDTBT/CdSe QDs films containing QDs modified with different benzenedithiols show various levels of PL quenching compared to the neat polymer film. Stronger PL quenching was observed when gradually lying down the benzene ring. Because the morphology of the hybrid films remains the same after the postdeposition ligand exchange process (Figure S5, Supporting Information),[22,33] the increased level of polymer PL quenching could be attributed to the enhanced electronic coupling between polymer and nanocrystals, facilitating the exciton dissociation process, which is prerequisite for achieving high efficient photovoltaic devices.[49−51] This PL quenching trend is in agreement with the mobility change trend discussed above, indicating the strongest electronic coupling effect between polymer and CdSe QDs when 1,4-BDT was used as face-on orientation suggested by the simulation.

During the device fabrication, in order to get rid of the effect of the second ligand on the blend film, the same ligand was used for ligand exchange on the CdSe QD hole-blocking layer. Due to the removal of the original surfactants such as oleic acid, the electron mobility of the CdSe layer was improved as discussed above, which is beneficial for electron extraction. Figure 4a shows the $J-V$ characteristics of HSCs with different

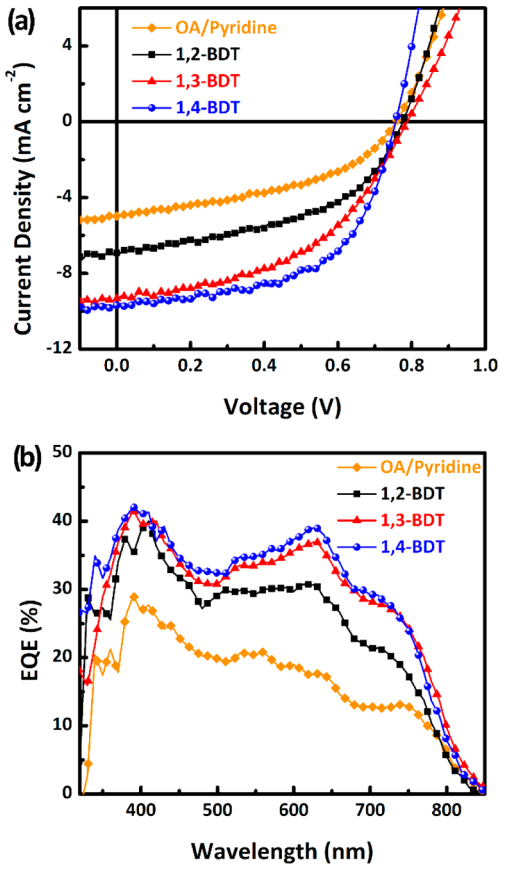

Figure 4. (a) $J-V$ characteristics of PCPDTBT/CdSe QDs HSCs with various orientated benzenedithiol at polymer/nanocrystal interface under simulated 1 sun AM 1.5 solar illumination. (b) Corresponding EQE of the devices.

benzenedithiols at the polymer/nanocrystal interface under simulated 1 sun AM 1.5 solar illumination. The photovoltaic performance parameters are also summarized in Table 1. Compared to the edge-on oriented 1,2-BDT, the face-on oriented 1,4-BDT results an increment in the J_{sc} from 6.77 ± 0.38 to 9.50 ± 0.20 mA cm^{-2} and FF from 0.466 ± 0.023 to

dx.doi.org/10.1021/am505130a | ACS Appl. Mater. Interfaces 2014, 6, 19154−19160

Table 1. Summary of Photovoltaic Performance of PCPDTBT:CdSe QDs HSCs with Various Orientated Benzenedithiol at Polymer/Nanocrystal Interface, Which Represent Statistical Averages of over 15 Devices for Each Configuration

Ligand	V_{OC} (V)	J_{SC} (mA cm^{-2})	FF (%)	PCE (%)	Rs (Ω cm^2)
OA/pyridine	0.77 ± 0.01	4.47 ± 0.19	42.8 ± 1.7	1.46 ± 0.11	27.4
EDT	0.76 ± 0.01	8.46 ± 0.25	47.1 ± 0.5	3.01 ± 0.05	
1,2-BDT	0.79 ± 0.02	6.77 ± 0.38	46.6 ± 2.3	2.49 ± 0.17	17.8
1,3-BDT	0.78 ± 0.01	8.66 ± 0.44	46.5 ± 1.4	3.16 ± 0.20	12.0
1,4-BDT	0.76 ± 0.01	9.50 ± 0.20	54.3 ± 1.8	3.92 ± 0.17	6.5

0.543 ± 0.018. Consequently, the face-on oriented benzene rings at the polymer/nanocrystal interface lead to the highest HSC performance with a PCE of 4.18% (3.92 ± 0.17%), which is 58% higher than that for devices with edge-on oriented ligands. We also fitted the dark-current density characteristics using the modified diode equation[52] including series resistance for the devices studied here. As summarized in Table 1, we see that the specific series resistance Rs is reduced from 17.8 to 12.0, and further to 6.5 Ω cm^2 as the orientation of the benzene ring change from edge-on to face-on fashion at the D/A interface. This reduction in series resistance agrees well with the enhanced charge transport properties discussed earlier (Figure 2).

The external quantum efficiency (EQE) spectra of these devices are shown in Figure 4b. It clearly shows that EQE was gradually improved in the entire spectral range when the benzenedithiols ligands turned to face-on from edge-on orientation. The improvement was more apparent in the range between 500 and 850 nm corresponding to the absorption of the polymer. This agrees well with the steady-state PL results described above, which showed that the face-on orientated benzene ring at the D/A interface improves the dissociation of excitons generated in the polymer into charges. Although there is only 10% PCPDTBT in weight or ∼30% in volume in the active layer of HSCs, the low band gap polymer contributes strongly to the light absorption due to its high absorption coefficient and its ability to harvest the near-infrared photons. These results are consistent with that the molecular face-on ordering relative to donor/acceptor (D/A) heterojunction interfaces could improve exciton dissociation and/or charge transport for polymer/fullerene based bulk heterojunction devices investigated.[53] Selecting or designing new ligands that favor face-on orientation on the surface of nanocrystals is critical for efficiently converting the long wavelength photons into electrons to achieve higher photocurrents. Recently, there has been a report on CdSe QD/reduced graphene oxide (rRO)-PCPDTBT hybrid films that achieved similar efficiencies. They found that V_{oc} was improved by 25−30% compared to the QD only devices mainly due to the higher electron mobility and reduction of trapped charges inside the active layer of rGO containing solar cells.[54] According to our results, the direct coupling of CdSe QD to a π-aromatic system in face-on orientation should also contribute to the improved performance.

To further confirm the significant effect of ligand orientation on the performance of HSCs, we also used three corresponding toluenethiols with only one −SH group to modify the D/A interface. *O*-toluenethiol, *m*-toluenethiol, *p*-toluenethiol with only one anchor group that cannot lie down on the surface of nanocrystals as 1,4-BDT does, which means the orientation of the benzene ring at the D/A interface cannot be tuned as the benzenedithiols. Figure 5 shows the *J*−*V* characteristic curves of PCPDTBT/CdSe QDs HSCs with various toluenethiols at

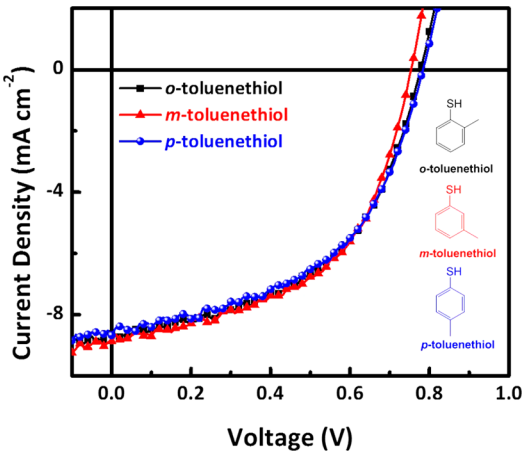

Figure 5. *J*−*V* characteristics of PCPDTBT/CdSe QDs HSCs with various toluenethiols at polymer/nanocrystal interface under simulated 1 sun AM 1.5 solar illumination.

polymer/nanocrystal interface and their device performances are summarized in Table 2. We can see that when these toluenethiols were used to treat the polymer/nanocrystal blend films, the HSC devices show very similar performance. And the PCE is less than the CdSe QD covered with 1,4-BDT. These results further demonstrate that the ligand orientation at the polymer/nanocrystal interface has a significant impact on the performance of HSCs, which has not been fully investigated before. Also as shown in Table 1, the device treated by 1,4-BDT showed much better performance than that treated by 1,2-ethanedithiol (EDT), indicating the "electroactive" π-orbitals of the BDT contribute to the performance improvement of HSCs.

4. CONCLUSIONS

In conclusion, the effects of ligand orientation on the charge transport properties of CdSe nanocrystals, the exciton dissociation process at the PCPDTBT/CdSe QDs interface and consequently the photovoltaic performance were systematically investigated. The orientation of benzenedithiol on CdSe QD surface was tuned by changing the substitution positions of the two thiols on the benzene ring as verified by DFT calculations. Making the "electroactive" benzene ring of benzenedithiol lie down on the QD surface can enhance the electronic coupling and to minimize the nanocrystal−nanocrystal or polymer−nanocrystal distance, thereby facilitating charge transport and exciton dissociation at the D/A interface. High performance hybrid solar cells based on PCPDTBT:CdSe QDs are demonstrated with a highest efficiency of 4.18% when 1,4-benzenedithiol is used for ligand exchange, which results in a face-on orientated benzene ring at the D/A interface. Although we have only focused on CdSe QDs in this work, our results show that judicious choice of ligands can enhance electronic coupling between donor and acceptor and greatly

Table 2. Summary of Photovoltaic Performance of PCPDTBT:CdSe QDs HSCs with Various Toluenethiols at the Polymer/Nanocrystal Interface

ligand	V_{OC} (V)	J_{SC} (mA cm^{-2})	FF (%)	PCE (%)
o-toluenethiol	0.79 ± 0.01	8.64 ± 0.20	51.9 ± 0.9	3.54 ± 0.11
m-toluenethiol	0.76 ± 0.01	8.85 ± 0.03	50.3 ± 3.3	3.34 ± 0.23
p-toluenethiol	0.78 ± 0.01	8.75 ± 0.16	50.8 ± 0.9	3.42 ± 0.07

improve the photovoltaic device performance. This research could open up a new pathway to improve further the performance of bulk heterojunction based hybrid solar cells that involve more efficient nanostructures, e.g., nanorods, and/or more advanced designs of conjugated polymers. These findings could also find use in further improving the performance of nanocrystal based devices such as FETs and LEDs.

■ ASSOCIATED CONTENT

Ⓢ Supporting Information

TEM image of CdSe QDs, FTIR and XPS for S 2s spectra of CdSe QDs films treated by different benzenethiols, synchrotron grazing-incidence small-angle X-ray scattering (GISAXS) patterns, and TEM images of PCPDTBT/CdSe nanocrystal blend films. This material is available free of charge via the Internet at http://pubs.acs.org.

■ AUTHOR INFORMATION

Corresponding Authors

*H. Chen. E-mail: hzchen@zju.edu.cn.
*H. Li. E-mail: hanying_li@zju.edu.cn.

Author Contributions

⊥These authors contributed equally. The paper was written through contributions of all authors. All authors have given approval to the final version of the paper.

Notes

The authors declare no competing financial interest.

■ ACKNOWLEDGMENTS

This work was supported by the Major State Basic Research Development Program (2014CB643503) and the National Natural Science Foundation of China (Grants 91233114, 51261130582 and 50990063). W. F. Fu and Ling Wang thank Yu Cao for the design of Figure 1a (schematic illustration of orientation of various benzenedithiols on the surface of CdSe QDs). W. F. Fu thanks Jun Ling for his helpful suggestions. J.Q. M, T.K. L and X. L acknowledge the financial support from CUHK Direct Grant No. 4053075.

■ REFERENCES

(1) Lee, J.-S.; Kovalenko, M. V.; Huang, J.; Chung, D. S.; Talapin, D. V. Band-like Transport, High Electron Mobility and High Photoconductivity in All-Inorganic Nanocrystal Arrays. *Nat. Nanotechnol.* **2011**, *6*, 348−352.

(2) Liu, Y.; Tolentino, J.; Gibbs, M.; Ihly, R.; Perkins, C. L.; Liu, Y.; Crawford, N.; Hemminger, J. C.; Law, M. PbSe Quantum Dot Field-Effect Transistors with Air-Stable Electron Mobilities above 7 cm^2 V^{-1} s^{-1}. *Nano Lett.* **2013**, *13*, 1578−1587.

(3) Qian, L.; Zheng, Y.; Xue, J.; Holloway, P. H. Stable and Efficient Quantum-Dot Light-Emitting Diodes Based on Solution-Processed Multilayer Structures. *Nat. Photonics* **2011**, *5*, 543−548.

(4) Sun, Q.; Wang, Y. A.; Li, L. S.; Wang, D.; Zhu, T.; Xu, J.; Yang, C.; Li, Y. Bright, Multicoloured Light-Emitting Diodes Based on Quantum Dots. *Nat. Photonics* **2007**, *1*, 717−722.

(5) Ip, A. H.; Thon, S. M.; Hoogland, S.; Voznyy, O.; Zhitomirsky, D.; Debnath, R.; Levina, L.; Rollny, L. R.; Carey, G. H.; Fischer, A.; Kemp, K. W.; Kramer, I. J.; Ning, Z.; Labelle, A. J.; Chou, K. W.; Amassian, A.; Sargent, E. H. Hybrid Passivated Colloidal Quantum Dot Solids. *Nat. Nanotechnol.* **2012**, *7*, 577−582.

(6) Tang, J.; Kemp, K. W.; Hoogland, S.; Jeong, K. S.; Liu, H.; Levina, L.; Furukawa, M.; Wang, X.; Debnath, R.; Cha, D.; Chou, K. W.; Fischer, A.; Amassian, A.; Asbury, J. B.; Sargent, E. H. Colloidal-Quantum-Dot Photovoltaics Using Atomic-Ligand Passivation. *Nat. Mater.* **2011**, *10*, 765−771.

(7) Seo, J.; Cho, M. J.; Lee, D.; Cartwright, A. N.; Prasad, P. N. Efficient Heterojunction Photovoltaic Cell Utilizing Nanocomposites of Lead Sulfide Nanocrystals and a Low-Bandgap Polymer. *Adv. Mater.* **2011**, *23*, 3984−3988.

(8) Huynh, W. U.; Dittmer, J. J.; Alivisatos, A. P. Hybrid Nanorod-Polymer Solar Cells. *Science* **2002**, *295*, 2425−2427.

(9) Ma, W.; Swisher, S. L.; Ewers, T.; Engel, J.; Ferry, V. E.; Atwater, H. A.; Alivisatos, A. P. Photovoltaic Performance of Ultrasmall PbSe Quantum Dots. *ACS Nano* **2011**, *5*, 8140−8147.

(10) Chen, Z.; Zhang, H.; Du, X.; Cheng, X.; Chen, X.; Jiang, Y.; Yang, B. From Planar-Heterojunction to n-i Structure: An Efficient Strategy to Improve Short-Circuit Current and Power Conversion Efficiency of Aqueous-Solution-Processed Hybrid Solar Cells. *Energy Environ. Sci.* **2013**, *6*, 1597−1603.

(11) Greaney, M. J.; Araujo, J.; Burkhart, B.; Thompson, B. C.; Brutchey, R. L. Novel Semi-Random and Alternating Copolymer Hybrid Solar Cells Utilizing CdSe Multipods as Versatile Acceptors. *Chem. Commun.* **2013**, *49*, 8602−8604.

(12) Zhou, R.; Zheng, Y.; Qian, L.; Yang, Y.; Holloway, P. H.; Xue, J. Solution-Processed, Nanostructured Hybrid Solar Cells with Broad Spectral Sensitivity and Stability. *Nanoscale* **2012**, *4*, 3507−3514.

(13) Jeltsch, K. F.; Schädel, M.; Bonekamp, J.-B.; Niyamakom, P.; Rauscher, F.; Lademann, H. W. A.; Dumsch, I.; Allard, S.; Scherf, U.; Meerholz, K. Efficiency Enhanced Hybrid Solar Cells Using a Blend of Quantum Dots and Nanorods. *Adv. Funct. Mater.* **2012**, *22*, 397−404.

(14) Peng, X.; Manna, L.; Yang, W.; Wickham, J.; Scher, E.; Kadavanich, A.; Alivisatos, A. P. Shape Control of CdSe Nanocrystals. *Nature* **2000**, *404*, 59−61.

(15) Peng, Z. A.; Peng, X. Formation of High-Quality CdTe, CdSe, and CdS Nanocrystals Using CdO as Precursor. *J. Am. Chem. Soc.* **2000**, *123*, 183−184.

(16) Böhm, M. L.; Kist, R. J. P.; Morgenstern, F. S. F.; Ehrler, B.; Zarra, S.; Kumar, A.; Vaynzof, Y.; Greenham, N. C. The Influence of Nanocrystal Aggregates on Photovoltaic Performance in Nanocrystal-Polymer Bulk Heterojunction Solar Cells. *Adv. Energy Mater.* **2014**, *4*, 1400139.

(17) Bouet, C.; Mahler, B.; Nadal, B.; Abecassis, B.; Tessier, M. D.; Ithurria, S.; Xu, X. Z.; Dubertret, B. Two-Dimensional Growth of CdSe Nanocrystals, from Nanoplatelets to Nanosheets. *Chem. Mater.* **2013**, *25*, 639−645.

(18) Wang, W.; Banerjee, S.; Jia, S.; Steigerwald, M. L.; Herman, I. P. Ligand Control of Growth, Morphology, and Capping Structure of Colloidal CdSe Nanorods. *Chem. Mater.* **2007**, *19*, 2573−2580.

(19) Fu, H.; Tsang, S.-W. Infrared Colloidal Lead Chalcogenide Nanocrystals: Synthesis, Properties, and Photovoltaic Applications. *Nanoscale* **2012**, *4*, 2187−2201.

(20) Jin, G.; Wei, H. T.; Na, T. Y.; Sun, H. Z.; Zhang, H.; Yang, B. High-Efficiency Aqueous-Processed Hybrid Solar Cells with an Enormous Herschel Infrared Contribution. *ACS Appl. Mater. Interfaces* **2014**, *6*, 8606−8612.

(21) Zhou, R.; Stalder, R.; Xie, D.; Cao, W.; Zheng, Y.; Yang, Y.; Plaisant, M.; Holloway, P. H.; Schanze, K. S.; Reynolds, J. R.; Xue, J. Enhancing the Efficiency of Solution-Processed Polymer:Colloidal Nanocrystal Hybrid Photovoltaic Cells Using Ethanedithiol Treatment. *ACS Nano* **2013**, *7*, 4846−4854.
(22) Celik, D.; Krueger, M.; Veit, C.; Schleiermacher, H. F.; Zimmermann, B.; Allard, S.; Dumsch, I.; Scherf, U.; Rauscher, F.; Niyamakom, P. Performance Enhancement of CdSe Nanorod-Polymer based Hybrid Solar Cells Utilizing a Novel Combination of Post-Synthetic Nanoparticle Surface Treatments. *Sol. Energy Mater. Sol. Cells* **2012**, *98*, 433−440.
(23) Nag, A.; Kovalenko, M. V.; Lee, J.-S.; Liu, W.; Spokoyny, B.; Talapin, D. V. Metal-Free Inorganic Ligands for Colloidal Nanocrystals: S^{2-}, HS^{-}, Se^{2-}, HSe^{-}, Te^{2-}, HTe^{-}, TeS_3^{2-}, OH^{-}, and NH_2^{-} as Surface Ligands. *J. Am. Chem. Soc.* **2011**, *133*, 10612−10620.
(24) Dong, A.; Ye, X.; Chen, J.; Kang, Y.; Gordon, T.; Kikkawa, J. M.; Murray, C. B. A Generalized Ligand-Exchange Strategy Enabling Sequential Surface Functionalization of Colloidal Nanocrystals. *J. Am. Chem. Soc.* **2010**, *133*, 998−1006.
(25) Webber, D. H.; Brutchey, R. L. Ligand Exchange on Colloidal CdSe Nanocrystals Using Thermally Labile tert-Butylthiol for Improved Photocurrent in Nanocrystal Films. *J. Am. Chem. Soc.* **2011**, *134*, 1085−1092.
(26) He, M.; Qiu, F.; Lin, Z. Toward High-Performance Organic-Inorganic Hybrid Solar Cells: Bringing Conjugated Polymers and Inorganic Nanocrystals in Close Contact. *J. Phys. Chem. Lett.* **2013**, *4*, 1788−1796.
(27) Williams, K. J.; Tisdale, W. A.; Leschkies, K. S.; Haugstad, G.; Norris, D. J.; Aydil, E. S.; Zhu, X. Y. Strong Electronic Coupling in Two-Dimensional Assemblies of Colloidal PbSe Quantum Dots. *ACS Nano* **2009**, *3*, 1532−1538.
(28) Yu, J.; Shen, T.-L.; Weng, W.-H.; Huang, Y.-C.; Huang, C.-I.; Su, W.-F.; Rwei, S.-P.; Ho, K.-C.; Wang, L. Molecular Design of Interfacial Modifiers for Polymer-Inorganic Hybrid Solar Cells. *Adv. Energy Mater.* **2012**, *2*, 245−252.
(29) Stalder, R.; Xie, D.; Zhou, R.; Xue, J.; Reynolds, J. R.; Schanze, K. S. Variable-Gap Conjugated Oligomers Grafted to CdSe Nanocrystals. *Chem. Mater.* **2012**, *24*, 3143−3152.
(30) Nam, M.; Kim, S.; Kim, S.; Kim, S. W.; Lee, K. Efficient Hybrid Solar Cells Using PbS_xSe_{1-x} Quantum Dots and Nanorods for Broad-Range Photon Absorption and Well-Assembled Charge Transfer Networks. *Nanoscale* **2013**, *5*, 8202−8209.
(31) Lek, J. Y.; Xi, L.; Kardynal, B. E.; Wong, L. H.; Lam, Y. M. Understanding the Effect of Surface Chemistry on Charge Generation and Transport in Poly(3-hexylthiophene)/CdSe Hybrid Solar Cells. *ACS Appl. Mater. Interfaces* **2011**, *3*, 287−292.
(32) Zhou, R.; Xue, J. Hybrid Polymer-Nanocrystal Materials for Photovoltaic Applications. *ChemPhysChem* **2012**, *13*, 2471−2480.
(33) Fu, W.; Shi, Y.; Qiu, W.; Wang, L.; Nan, Y.; Shi, M.; Li, H.; Chen, H. High Efficiency Hybrid Solar Cells Using Post-Deposition Ligand Exchange by Monothiols. *Phys. Chem. Chem. Phys.* **2012**, *14*, 12094−12098.
(34) Greaney, M. J.; Das, S.; Webber, D. H.; Bradforth, S. E.; Brutchey, R. L. Improving Open Circuit Potential in Hybrid P3HT:CdSe Bulk Heterojunction Solar Cells via Colloidal tert-Butylthiol Ligand Exchange. *ACS Nano* **2012**, *6*, 4222−4230.
(35) Wu, Y.; Zhang, G. Performance Enhancement of Hybrid Solar Cells Through Chemical Vapor Annealing. *Nano Lett.* **2010**, *10*, 1628−1631.
(36) Stolle, C. J.; Panthani, M. G.; Harvey, T. B.; Akhavan, V. A.; Korgel, B. A. Comparison of the Photovoltaic Response of Oleylamine and Inorganic Ligand-Capped $CuInSe_2$ Nanocrystals. *ACS Appl. Mater. Interfaces* **2012**, *4*, 2757−2761.
(37) Zhitomirsky, D.; Furukawa, M.; Tang, J.; Stadler, P.; Hoogland, S.; Voznyy, O.; Liu, H.; Sargent, E. H. N-Type Colloidal-Quantum-Dot Solids for Photovoltaics. *Adv. Mater.* **2012**, *24*, 6181−6185.
(38) Qian, L.; Yang, J.; Zhou, R.; Tang, A.; Zheng, Y.; Tseng, T.-K.; Bera, D.; Xue, J.; Holloway, P. H. Hybrid Polymer-CdSe Solar Cells with a ZnO Nanoparticle Buffer Layer for Improved Efficiency and Lifetime. *J. Mater. Chem.* **2011**, *21*, 3814−3817.
(39) Kresse, G.; Hafner, J. *Ab Initio* Molecular Dynamics for Liquid Metals. *Phys. Rev. B* **1993**, *47*, 558−561.
(40) Kresse, G.; Furthmüller, J. Efficiency of *Ab-Initio* Total Energy Calculations for Metals and Semiconductors Using a Plane-Wave Basis Set. *Comput. Mater. Sci.* **1996**, *6*, 15−50.
(41) Perdew, J. P.; Burke, K.; Ernzerhof, M. Generalized Gradient Approximation Made Simple. *Phys. Rev. Lett.* **1996**, *77*, 3865−3868.
(42) Blöchl, P. E. Projector Augmented-Wave Method. *Phys. Rev. B* **1994**, *50*, 17953−17979.
(43) Cho, S. H.; Han, H. S.; Jang, D.-J.; Kim, K.; Kim, M. S. Raman Spectroscopic Study of 1,4-Benzenedithiol Adsorbed on Silver. *J. Phys. Chem.* **1995**, *99*, 10594−10599.
(44) Joo, S. W.; Han, S. W.; Kim, K. Adsorption of 1,4-Benzenedithiol on Gold and Silver Surfaces: Surface-Enhanced Raman Scattering Study. *J. Colloid Interface Sci.* **2001**, *240*, 391−399.
(45) Barron, H.; Fernández-Seivane, L.; López-Lozano, X. Systematic Study of the Adsorption of Thiol Molecules on a Au55 Nanoparticle. *Phys. Status Solidi B* **2014**, *251*, 1239−1247.
(46) da Silva Filho, D. A.; Kim, E. G.; Brédas, J. L. Transport Properties in the Rubrene Crystal: Electronic Coupling and Vibrational Reorganization Energy. *Adv. Mater.* **2005**, *17*, 1072−1076.
(47) Sirringhaus, H.; Brown, P. J.; Friend, R. H.; Nielsen, M. M.; Bechgaard, K.; Langeveld-Voss, B. M. W.; Spiering, A. J. H.; Janssen, R. A. J.; Meijer, E. W.; Herwig, P.; de Leeuw, D. M. Two-Dimensional Charge Transport in Self-Organized, High-Mobility Conjugated Polymers. *Nature* **1999**, *401*, 685−688.
(48) Yang, J.; Tang, A.; Zhou, R.; Xue, J. Effects of Nanocrystal Size and Device Aging on Performance of Hybrid Poly(3-hexylthiophene):CdSe Nanocrystal Solar Cells. *Sol. Energy Mater. Sol. Cells* **2011**, *95*, 476−482.
(49) Bin, Y.; Yongbo, Y.; Pankaj, S.; Shashi, P.; Rafal, K.; Stephen, D.; Alexei, G.; Ravi, S.; Jinsong, H. Tuning the Energy Level Offset between Donor and Acceptor with Ferroelectric Dipole Layers for Increased Efficiency in Bilayer Organic Photovoltaic Cells. *Adv. Mater.* **2012**, *24*, 1455−1460.
(50) Schiros, T.; Kladnik, G.; Prezzi, D.; Ferretti, A.; Olivieri, G.; Cossaro, A.; Floreano, L.; Verdini, A.; Schenck, C.; Cox, M.; Gorodetsky, A. A.; Plunkett, K.; Delongchamp, D.; Nuckolls, C.; Morgante, A.; Cvetko, D.; Kymissis, I. Donor-Acceptor Shape Matching Drives Performance in Photovoltaics. *Adv. Energy Mater.* **2013**, *3*, 894−902.
(51) Mattioli, G.; Dkhil, S. B.; Saba, M. I.; Malloci, G.; Melis, C.; Alippi, P.; Filippone, F.; Giannozzi, P.; Thakur, A. K.; Gaceur, M.; Margeat, O.; Diallo, A. K.; Videlot-Ackermann, C.; Ackermann, J.; Bonapasta, A. A.; Mattoni, A. Interfacial Engineering of P3HT/ZnO Hybrid Solar Cells Using Phthalocyanines: A Joint Theoretical and Experimental Investigation. *Adv. Energy Mater.* **2014**, DOI: 10.1002/aenm.201301694.
(52) Yang, F.; Shtein, M.; Forrest, S. R. Controlled Growth of a Molecular Bulk Heterojunction Photovoltaic Cell. *Nat. Mater.* **2005**, *4*, 37−41.
(53) Tumbleston, J. R.; Collins, B. A.; Yang, L.; Stuart, A. C.; Gann, E.; Ma, W.; You, W.; Ade, H. The Influence of Molecular Orientation on Organic Bulk Heterojunction Solar Cells. *Nat. Photonics* **2014**, *8*, 385−391.
(54) Eck, M.; Pham, C. V.; Zufle, S.; Neukom, M.; Sessler, M.; Scheunemann, D.; Erdem, E.; Weber, S.; Borchert, H.; Ruhstaller, B.; Kruger, M. Improved Efficiency of Bulk Heterojunction Hybrid Solar Cells by Utilizing CdSe Quantum Dot-Graphene Nanocomposites. *Phys. Chem. Chem. Phys.* **2014**, *16*, 12251−12260.